Field emission from as-grown and surface modified BN and CN thin films

N. Badi, A. Tempez, D. Starikov, and A. Bensaoula[a)]
Nitride Materials and Devices Laboratory, SVEC, The University of Houston, Houston, Texas 77204-5507

V. P. Ageev, A. Karabutov, M. V. Ugarov, V. Frolov, and E. Loubnin
Natural Sciences Center of General Physics Institute, Moscow, Russia 117942

K. Waters and A. Shultz
Ionwerks, 2472 Bolsover, Suite 255, Houston, Texas 77005

(Received 2 November 1998; accepted 15 March 1999)

We have investigated the electron field emission characteristics of BN and CN on highly conductive silicon thin films deposited by End-Hall ion source and electron cyclotron resonance plasma source-assisted physical vapor deposition. The thermal processing and surface laser modification effects on the field emission properties were investigated. Current density-field emission characteristics $I_\eta(E)$ were tested in a high vacuum environment. Mg-doped BN thin films on silicon exhibited a turn-on field as low as 25 V/μm and a current density higher than 1 A/cm^2. The deposition of a thin BN layer on copper lithium (CuLi) metallic substrate yields surfaces with a 75 V/μm onset field and a current density 1000 times higher than that obtained from uncoated surfaces. Under high vacuum laser annealing BN coated CuLi showed no enhancement but more stable emission characteristics. Our results show also that pulsed ultraviolet laser irradiation of CN films in vacuum results in an increase of the field emission current densities and a reduction in threshold field values. The turn-on fields of the irradiated surfaces depend strongly upon the energy density of the laser beam. In addition, the electroconductivity properties of BN and CN surface mapping have been performed using scanning tunneling field emission microscopy. The surface topography mapping and its correlation to the field emission properties were investigated. Preliminary results on surface mapping suggest that the surface relief plays some role in field emission enhancement.
 [S0734-2101(99)14704-3]

I. INTRODUCTION

In vacuum microelectronics and field emission displays applications it is very important to employ systems having high emission currents at sufficiently low applied voltages. One approach is to cover the cathodes with a thin layer of material (i.e., diamond) of low work function (about 4.5 eV) so that field emission is obtained at low applied voltage.[1]

In spite of their very promising prospect,[2–5] the diamond-based field emitters are still suffering from problems such as high growth temperature and poor uniformity. The hydrogenation and oxidation of diamond films in energetically active/corrosive gaseous environments prohibits their application as cold cathode materials for low vacuum ion and electron sources. This requirement is also an obstacle to realizing the potential efficiency of diamond-based cold cathodes and sensors.

Diamond-like amorphous carbon (DLC) films require higher voltage to initiate the emission and their emission current densities are lower than those from diamond emitters. As an alternative material for field emission effect devices, BN is chemically and thermally stable and exhibits a negative electron affinity (NEA) effect that is recognized as a major factor responsible for its electron field emission properties. However, NEA is also inherent to other wide band gap materials such as LiF[6] and CaF_2.[7] The first observation of a NEA in boron nitride crystals and thin films was reported in 1958.[8] The presence of NEA was determined by ultraviolet photoemission spectroscopy. The electron emission from carbon-doped boron nitride was reported by Pryor[9,10] in 1996.

In this article, electron field emission from BN and CN coatings is investigated. The conductivity properties of BN and CN surfaces have been performed using scanning tunneling field emission microscopy (STFEM).[11–13] Field emission enhancement, stability of the thin film surface, and surface modification under high vacuum thermal and laser annealing are reported.

II. EXPERIMENTS

Prior to deposition, high conductivity silicon (100 *n* type) and CuLi substrates were degreased using standard solvents, rinsed in de-ionized (DI) water and dried with nitrogen. The substrates were cleaned *in situ* under argon bombardment for 10 min.

BN and CN thin films (25–300 nm thickness) were grown in a high vacuum reactor equipped with an Auger spectrometer. High purity boron and carbon were evaporated by electron beams and controlled at 0.2 Å/s by a quartz crystal monitor rate. Both an End-Hall ion source (Mark II) and an electron cyclotron resonance (ECR) ASTEX plasma source were used for nitrogen species delivery. The ion beam energy/current in the End-Hall ion source were fixed at 45 eV/110 mA. The N_2 flow through the ECR source varied from 2 to 5 sccm and the power of the ECR was maintained

a)Electronic mail: Bens@space.svec.uh.edu

at 75 W. The growth temperatures ranged from 400 to 600 °C for BN/Si and ~80 °C for BN on CuLi and CN/Si film deposition. The pressure during deposition was 10^{-5} Torr using the End-Hall ion source and 10^{-4} Torr for the ECR plasma source. *In situ* Auger electron spectroscopy (AES) measurements were performed to check the cleanliness of the substrates prior to deposition and to determine the postgrowth surface composition.

Field emission characteristics were studied in a high vacuum chamber with a pressure below 10^{-7} Torr. Four tungsten tip probes (anodes) with 20 μm curvature radii were place at a distance of 10–100 μm from the sample surface (cathode). A high dc voltage of up to 8 kV was applied between the sample and each probe separately to induce field emission. The measurement procedure included recording of the emission current during the automated increasing–decreasing cycles of the electrical field. The emission current density was calculated by dividing the measured current by the total surface area of the four tips used.

The correlation between the surface relief, electron field emission and surface electroconductivity of the BN and CN surfaces have been performed using STFEM. This mapping technique is based on the registration of the electron current I_t through the vacuum gap d_t between a sample surface and a probe at a stable applied voltage. The total spatial resolution of this technique was as high as a few nm. There are two main registration modes in STFEM. In the first mode the current I_t is maintained constant at the value of I_0 by automatic change of probe position normally to the sample surface, i.e., in the Z direction (''relief'' mode). In this case the signal is the voltage on the Z-axis manipulator electrode, which is proportional to the normal shift of the probe. The ''relief'' mode magnitude is defined by two components: surface relief height and vacuum gap d_t, depending on the probability of electron tunneling through the surface potential barrier. For the second mode (so called ''spectrum'' mode) the probe vibrates normally to the sample surface with a low amplitude at a frequency up to 100 kHz. The ac current component value is proportional to the effective surface electron potential.[13] The term ''surface electron potential'' is used instead of ''electron work function.'' The reason is that the electron work function alone does not determine the value of the potential barrier for electron emission from low doped (high resistivity) semiconductor materials. There is also, for example, the surface concentration of impurity centers which plays an important role. In a highly conducting material the surface potential is practically identical to the work function.

The following procedure was used to study the emission centers in our materials. Both ''relief'' and ''spectrum'' modes can be acquired simultaneously in a single scan. The scanning area is divided in $N\times N$ (64×64 or 128×128 in our case) points. At each point the signals are measured at different bias voltages U_b (negative for sample-to-probe current direction, and positive for the reverse) except for the ''forbidden'' voltage range $0\leqslant|U_b|\leqslant U_{\min}$. It must be emphasized that a correct STFEM measuring environment is provided only if the applied voltage U_b prevails over the voltage drop $U_s=I_t/G_s$ during scanning: $|U_b|>U_{\min}=I_0/G_{\min}$ ($G_{\min}$ is the minimum value of local electroconductivity G_s). In the ''forbidden'' voltage range the current I_t through some points of the scanned area is too small to hold the constant value of I_0 even when the probe is in contact with the sample. Hence, as a preliminary step, a series of scans with decreasing value of $|U_b|$ is made until a ''spectrum'' mode signal for a certain low conducting region on the scanned area is saturated at an extreme high level. It means that the probe is nearly in contact with this region. Owing to this procedure the correct measuring conditions $|U_b|>U_{\min}=I_0/G_{\min}/G_{\min}$ ($G_{\min}$ is the minimum value of local electroconductivity G_s for the scanned area) are determined. The values of $U_{\min}$ at positive and negative polarities depend on the physical properties of the material, particular on its surface conductivity and electron band structure. At the end of the measurements, the following maps of an area can be produced:

(a) A map based on the ''relief'' mode measured at low bias voltages. This map gives an information about surface topology.
(b) A map based on ''relief'' mode measured at high negative bias voltages. Such a map contains a general information about surface topology and electron emission.
(c) ''Spectrum'' maps, at low negative and positive bias voltages, give information about surface potential distribution (surface electroconductivity).

Two ''relief'' maps, at low and at high negative voltages, may be point-by-point subtracted from each other to obtain the distribution of the electron emission component. The resulting map shows the positions of emission centers so that higher magnitude peaks in such ''emission'' maps are associated with more intense emission centers.

The comparison of ''relief,'' ''emission'' and ''surface potential'' maps allows one to study the correlation between geometrical, field electron emission and the conduction properties of the sample surface.

In the surface modification experiments, a pulsed excimer KrF laser (248 nm, $h\nu=5.0$ eV) was used as a radiation source. The pulse energy was increased to up to 100 mJ; the pulse duration was 20 ns with a pulse repetition rate up to 1000 Hz. Irradiation was performed in a high vacuum chamber with a base pressure of 10^{-8} Torr. The film surface was held at room temperature. A two-lens optical projection scheme with an intermediate diaphragm was applied to provide a uniform surface illumination of a spot area of ~1 mm^2. It was necessary to make a 4×4 matrix of laser spots to provide an area sufficient for field emission measurements. The intensity of the laser radiation was chosen below the value that led to visible alteration of the thin film surface.

III. RESULTS

A. Boron nitride on silicon films

Figure 1 shows the field emission characteristics from undoped 250 Å BN film (BN58) grown at 520 °C using an ECR

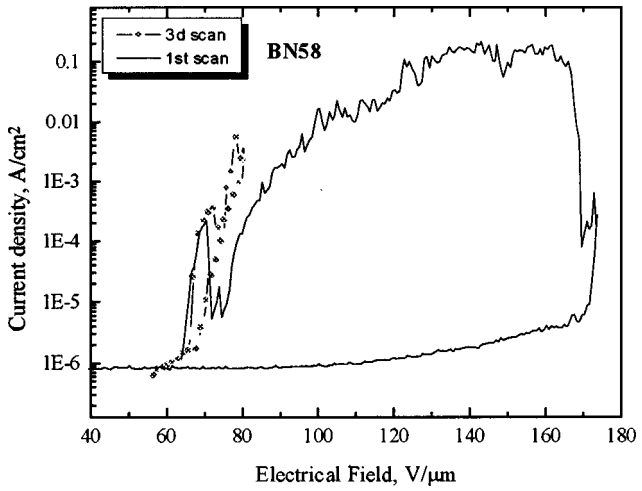

FIG. 1. Field emission characteristics obtained from undoped 250 Å BN film (BN58) grown at 520 °C using an ECR plasma source and a 4 sccm nitrogen flow.

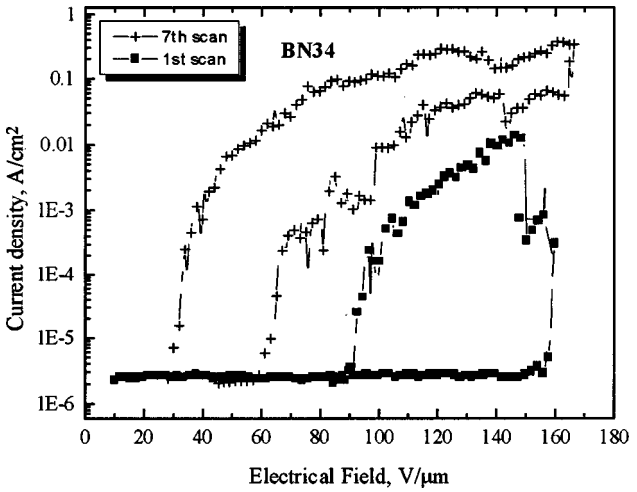

FIG. 2. Field emission characteristics obtained from Mg-doped BN sample (BN34) grown at 450 °C using an End-Hall ion source (45 eV, 110 mA).

plasma source under a 4 sccm nitrogen flow. There is a significant difference in $I_\eta(E)$ behavior between the first and the subsequent cycles (only first and third cycles are shown here). The first cycle exhibits a nonzero current before a well-distinguished electrical breakdown of the films takes place, resulting in an uncontrollable jump of the emission current by a few orders of magnitude. The subsequent reduction of the electrical field within a frame of the same cycle is accompanied by the decrease of the electrical current. The electrical field values on the film surface at the breakdown thresholds are on the order of 100 V/μm which to some extent depend on film structure and film thickness.

For the next cycles, the $I_\eta(E)$ curves exhibited a tendency to a smooth current increase above a critical value of the applied field which may be interpreted as an emission threshold of ''modified'' films. This is most likely a result of the observed electrical breakdown. The improvement of the emission with the number of scans is probably due to a surface reconditioning with the increase and decrease of the electric field. We noticed that the emission threshold becomes significantly lower with the cycle number. The hysteresis of the emission current becomes less significant with the number of the field cycling.

Similar features, with a relatively lower emission electric field threshold, were observed in films grown using the End–Hall ion source. Figure 2 shows a typical spectrum for relatively thicker (~120 nm) Mg-doped BN thin films (BN34) grown at 450 °C. The turn-on field is lower and stabilizes around 25 V/μm after the seventh cycle. However, the corresponding emission characteristics remain below those of typical chemical vapor deposition (CVD) diamond films. With the exception of the two samples mentioned above (BN58 and BN34), we have to underline the similarity of the emission behavior for the BN films grown under different conditions.

STFEM investigation of a 400×400 nm^2 area from a typical BN/Si sample reveals discrete electrically conducting inclusions 10–50 nm in size. The local electrical conductivity values of the high resistivity areas are evaluated to be lower than $G<0.03$ nS. Under the same conditions, larger features of 100–200 nm were observed for samples with a higher nitrogen concentration and having similar local electrical conductivity values.

B. Boron nitride on CuLi

Figure 3 shows field emission characteristics from BN coated and uncoated CuLi substrates. The boron nitride thin film coatings were deposited by ECR (75 W; $N_2=4$ sccm) at near room temperature. Using BN coatings results in an enhancement of the field emission current density by 3 orders of magnitude ($\times 10^3$) and a lowering of the emission threshold field by a factor of 2. The turn-on field of the bare substrates was 150 V/μm and the maximum current density was

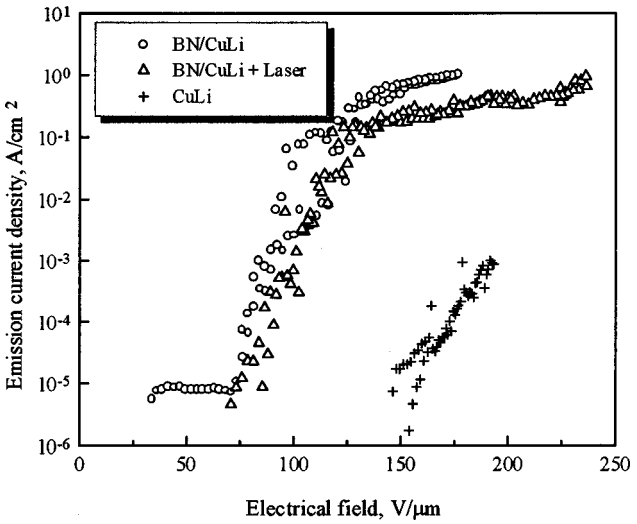

FIG. 3. Field emission characteristics from BN coated and uncoated CuLi. The BN were deposited at ~80 °C using an ECR and a 4 sccm nitrogen flow.

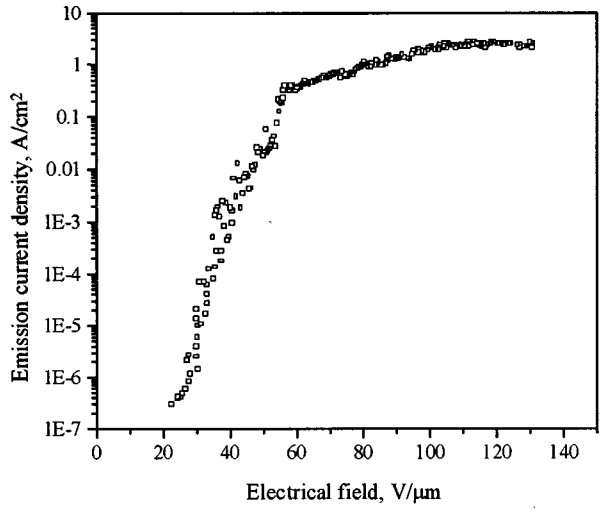

FIG. 4. Field emission characteristics from BN coated CuLi sample grown at ~80 °C using an End-Hall ion source (45 eV, 110 mA).

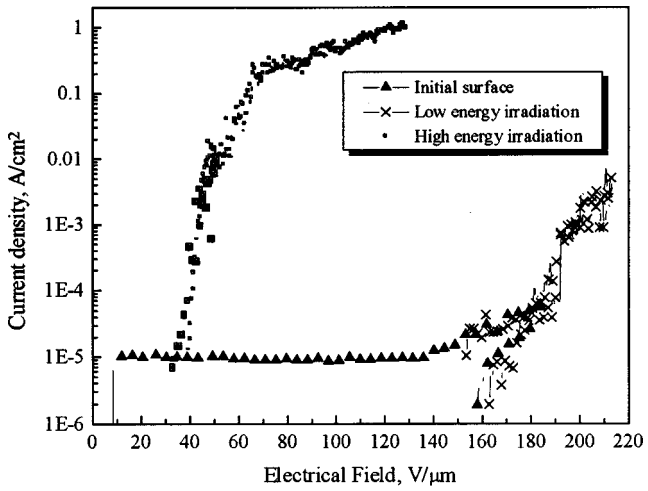

FIG. 5. Field emission characteristics from CN sample grown at room temperature before and after pulsed excimer KrF laser (248 nm) irradiation.

1 mA/cm^2. The turn-on field of the BN coated substrates was 75 V/μm and a maximum current density of 1 A/cm^2 at 175 V/μm.

Similar samples with BN coatings deposited using the End–Hall ion source show a turn-on field as low as 30 V/μm and a maximum current density exceeding 2 A/cm^2 at 100 V/μm (Fig. 4). A 200×200 nm^2 area from the same sample was investigated by STFEM. Low conducting inclusions were observed with lateral sizes of 20–50 nm and local electroconductivity of 0.3 nS. High resistivity BN areas are found primarily in the valleys of the surface relief, but emission centers (peaks on the emission profiles) occur near the boundary of the high resistivity–low resistivity area. A higher degree of surface electroconductivity inhomogeneity, associated with the relief details of the surface, was observed for films grown on CuLi substrates. The large difference observed between thresholds of BN films grown on CuLi and Si is probably due to: (i) the original surface roughness of a CuLi substrate compared to that of silicon wafer: (ii) lithium which is well known to lower the work function in alkali metal–alloy coatings.

Under high vacuum annealing, uncoated CuLi samples showed a rapid deterioration of the emission current, while BN coated CuLi samples showed stable emission characteristics.

Figure 3 also shows the results of laser vacuum annealing of the previously described samples using a KrF excimer laser (248 nm). The irradiation was performed in a series of 1000 pulses using a power intensity slightly lower than that leading to a visible alteration of the film surface. No visible enhancement of the current density was observed for either uncoated or coated CuLi surfaces except that the field emission behavior becomes smoother and more stable.

C. Carbon nitride on silicon films

The effect of laser irradiation on the electron field emission properties of CN thin film is presented next. Typical dependencies of the emission current upon applied field for the surface before and after irradiation are given in Fig. 5. The hysteresis-like curves represent the behavior at increasing and decreasing fields. A significant decrease of the emission electric field threshold (about 40 V/μm) and a higher current density, exceeding 1 A/cm^2 was obtained at a laser energy density of 0.2 J/cm^2. STFEM investigation of 400 ×400 nm^2 reveals inclusions with a size of 100–150 nm. This particular CN film had a 25% N surface composition as measured during deposition by AES. Emission centers (peaks on the emission profiles) occur near the boundary of the high resistivity–low resistivity areas. This is similar to the case of BN/CuLi samples. The local electrical conductivity values of the high resistivity areas were evaluated to be $G=0.2$ nS. Another sample with a 32% nitrogen content shows conductive inclusions with sizes of 50–150 nm. The local electrical conductivity values of the high resistivity areas were as high as $G=0.08$ nS.

The above results are important for cold cathode device development. Beside the electron affinity process mentioned in the literature for wide gap materials and the band gap states generated by defects such as vacancies and grain boundaries in CVD diamond films,[14] it is shown here that the presence of a high surface density of high and low electrical resistivity areas plays an important role in the field emission characteristics of a surface.

Table I presents the results of x-ray photoelectron spec-

TABLE I. X-ray photoelectron spectroscopy analysis of a series of irradiated CN surface spots.

Spot No.	Power density (J/cm^2)	sp^2 Fraction (%)	N[1]/N[2] ratio	N_2 (%)	O_2 (%)	Si
1	initial surface	83	1.1	10%–11%	<2	···
2	0.05	90	0.7	7%–8%	<1	traces
3	0.10	87	0.3	7%–8%	<1	···
4	0.20	95	0.3	5%–6%	<1	much

troscopy analysis of a series of irradiated surface spots from CN thin films. The bonding energies of the C^{1s} and N^{1s} spectral lines of the original film surface corresponded to the typical values for CN films found in the literature. The bonding energies for the doublet N^{1s} peak were 398.2 eV (peak N[1]) and 400 eV (peak N[2]). The ratio of the peak intensities was equal to 1.1 for an atomic nitrogen concentration of 10%–11% and an oxygen contamination up to 2%.

The laser irradiation effectively changes the surface composition of the CN_x films. The nitrogen concentration decreased by about 50% with respect to the original value after irradiation with a beam energy of 0.20 J/cm^2. The oxygen concentration in the modified layers did not exceed 0.2%–0.3% (much less that the original value) and remained the same after long exposure to the atmosphere at room temperature.

The detailed analysis of the C^{1s} lines showed that the bond energies depend strongly on irradiation power density and shift toward the values characteristic of graphite (284.1–284.3 eV). The shape of the C^{1s} line was found to be asymmetric without any visible multiplet structure.

The increase of the sp^2 bonding fraction (graphitization) is also supported by our analysis of the electronic structure of the irradiated CN_x films. As the laser radiation power increases this fraction goes up to 95% at 0.2 J/cm^2. As seen in Table I the intensity of the N[2] peak also increases. This peak is attributed to nontetrahedral coordination of nitrogen atoms in CN_x film.

IV. CONCLUSION

Field emission studies have been performed on BN and CN films deposited on high conductivity silicon substrates by End-Hall ion and ECR plasma source-assisted physical vapor deposition. As-grown thinner BN and relatively thicker Mg-doped BN films exhibited a turn-on field as low as 25 V/μm and a current density of about 1 A/cm^2.

The turn-on field of CuLi coated BN sample was 75 V/μm with a maximum current density 1000 times higher than those from uncoated CuLi samples. Under high vacuum laser annealing BN coated CuLi showed no enhancement but more stable emission characteristics.

The main result from CN thin films laser treatment experiments is the clear change in the surface atomic and chemical composition with the increase of the laser radiation power density. The nitrogen content and the fraction of sp^3 C–N and N–N bonding diminish after irradiation. This effect is accompanied by an enhancement of the electron emission properties of the irradiated areas. The maximum sp^2 bonding fraction (95%) corresponds to the lowest emission threshold.

As far as surface electroconductivity mapping, the important results are that the higher emission currents and lower thresholds are observed for films with high inhomogeneity in surface electroconductivity values that are associated with the details of the surface relief. The high resistivity areas are accumulated primarily in valleys, and the emission centers (peaks on the emission profiles) are placed near the boundaries between high and low resistivity areas. In the case of BN and CN thin films deposited on Si, the surface appears to be smoother and a good emission current is usually observed only after electrical breakdown.

ACKNOWLEDGMENTS

This work was supported by funds from a NASA cooperative agreement Grant No. NCC8-127 to SVEC, a Texas Advanced Technology Program Grant No. 1-1-32061. Ionwerks would like to acknowledge support from U.S. Air Force SBIR Contract No. F33615-97-C-1035 monitored by Dr. J. E. Van Nostrand; and a NASA phase II SBIR Grant No. NASA-9701 through MSFC monitored by Dr. Jerry Watkins. This material is also based upon work supported by the U.S. Civilian Research and Development Foundation under Award No. REI-247. All the authors would like to acknowledge Dr. A. Kraus and O. Auciello from Argonne National Laboratory for supplying the CuLi samples.

[1]R. B. Marcus, T. S. Ravi, T. Gmitter, H. H. Busta, J. T. Nicuum, K. K. Chin, and D. Liu, IEEE Trans. Electron Devices **ED-38**, 2289 (1991).
[2]C. Wang, A. Garcia, D. C. Ingram, M. Lake, and M. E. Kordesch, Electron. Lett. **27**, 1459 (1991).
[3]N. S. Xu, R. V. Latham, and Y. Tzeng, Electron. Lett. **29**, 1596 (1993).
[4]W. Zhu, G. P. Kochanski, S. Jin, and L. Seibles, J. Vac. Sci. Technol. B **14**, 2011 (1996).
[5]K. Okano, S. Koizumi, S. R. P. Silva, and G. A. J. Amaratunga, Nature (London) **381**, 140 (1996).
[6]D. A. Laoiano-Smith, E. A. Eklund, F. J. Himpsel, and L. J. Terminello, Appl. Phys. Lett. **59**, 2174 (1991).
[7]R. T. Poole, D. R. William, J. D. Riley, J. G. Jenkin, J. Liesegang, and R. C. G. Leckey, Chem. Phys. Lett. **36**, 401 (1975).
[8]M. J. Powers, M. C. Benjamin, L. M. Porter, R. J. Nemanich, and R. F. Davis, Appl. Phys. Lett. **67**, 3912 (1995).
[9]R. W. Pryor, Appl. Phys. Lett. **68**, 1802 (1996).
[10]R. W. Pryor, Mater. Res. Soc. Symp. Proc. **416**, 425 (1996).
[11]A. V. Karabutov, V. I. Konov, S. M. Pimenov, E. D. Obraztsova, V. D. Frolov, V. G. Pereverzev, and A. A. Smolin, 8th European Conference on Diamond, Diamond-like and Related Materials, Edinburgh, Scotland, August 3–8, 1997, paper No. 15.125; Diamond Relat. Mater. (in press).
[12]A. V. Karabutov, V. I. Konov, V. G. Ralchenko, E. D. Obraztsova, V. D. Frolov, S. A. Uglov, H.-J. Scheibe, V. E. Streinitskij, and V. I. Polyakov, Diamond Relat. Mater. **7**, 802 (1998).
[13]V. D. Frolov, A. V. Karabutov, V. I. Konov, S. M. Pimenov, and A. M. Prokhorov, J. Phys. D: Appl. Phys. **32**, 815 (1999).
[14]Z. Huang, P. H. Cutler, N. M. Miskovsky, and T. E. Sullivan, Appl. Phys. Lett. **65**, 2562 (1994); J. Vac. Sci. Technol. B **13**, 1 (1995).